Stress granules affect the sensitivity of renal cancer cells to sorafenib by sequestering and stabilizing COX-2 mRNA

HUIQI DAI[1,2*], GUOLI WANG[1,2*], WENMIN CAO[2], WEI QI[2,3], WEI CHEN[1,2] and HONGQIAN GUO[1,2]

[1]Department of Urology, Nanjing Drum Tower Hospital Clinical College of Nanjing University of Chinese Medicine; [2]Department of Urology, Nanjing Drum Tower Hospital, The Affiliated Hospital of Nanjing University Medical School, Institute of Urology Nanjing University, Nanjing, Jiangsu 210008; [3]Department of Urology, The Second People's Hospital of Hefei, Hefei, Anhui 230001, P.R. China

Received December 24, 2022; Accepted April 25, 2023

DOI: 10.3892/ol.2023.13860

Abstract. Most patients with renal cancer will develop resistance to sorafenib therapy and will therefore exhibit disease progression. Effective therapies for these patients are extremely limited. Cyclooxygenase-2 (COX-2) promotes the malignant transformation of cancer cells and drug resistance. The potential of COX-2 inhibitor (celecoxib) administration in combination with sorafenib for the treatment of renal cancer is unclear. The present study demonstrated that sorafenib rapidly increased the expression of COX-2 in renal cancer cells, as determined using reverse transcription-quantitative PCR and western blotting. The results of the MTT assay and cell apoptosis experiment demonstrated that the cytotoxicity of sorafenib was also affected by COX-2 expression and celecoxib enhanced the cytotoxicity of sorafenib against renal cell carcinoma. Immunofluorescence analysis indicated that sorafenib induced the formation of stress granules (SGs) in renal cancer cells. In addition, COX-2 expression was associated with the formation of SGs, and SGs could capture and stabilize COX-2 mRNAs in renal cancer cells; this was confirmed using RNA fluorescence *in situ* hybridization and an actinomycin D chase experiment. The protective effect of SGs was further demonstrated in cell experiments and xenograft tumor models. Thus, the present study indicated that the use of celecoxib may significantly enhance the sensitivity of renal cancer cells to sorafenib and improve efficacy. Sorafenib-induced SGs may contribute to critical events that promote COX-2 expression and survival in renal cancer cells. Therefore, the present study may provide novel ideas for the treatment of renal cancer.

Correspondence to: Professor Hongqian Guo or Dr Wei Chen, Department of Urology, Nanjing Drum Tower Hospital Clinical College of Nanjing University of Chinese Medicine, 321 Zhongshan Road, Nanjing, Jiangsu 210008, P.R. China
E-mail: dr.ghq@nju.edu.cn
E-mail: chenw@njglyy.com

*Contributed equally

Key words: renal cancer, sorafenib, celecoxib, cyclooxygenase-2, stress granule

Introduction

The incidence of renal cell carcinoma (RCC) is increasing (1,2). Approximately one in five patients with RCC miss surgery at the time of diagnosis, and almost one in three patients with localized RCC will have recurrence after resection, these patients have a 5-year survival rate of <10% and are not sensitive to radiation or chemotherapy (3). Tyrosine kinase inhibitors (TKIs) are the main treatment choice for advanced renal cancer. Sorafenib is the first multi-target TKI approved for the treatment of renal cancer with dual antitumor activity. Sorafenib has direct antitumor activities by inhibiting RAF/MEK/ERK signaling, and it also acts on VEGFR, platelet-derived growth factor (PDGFR) and other targets to inhibit tumor angiogenesis (4). However, some patients with RCC do not respond sufficiently to sorafenib treatment, and most patients develop resistance and disease progression over time, even if sorafenib is initially effective (5). Therefore, there is an urgent need to elucidate the underlying mechanisms of sorafenib sensitivity regulation and to explore effective strategies to improve clinical diagnosis and treatment of renal cancer.

Cyclooxygenase-2 (COX-2) has low expression in normal cells, but high expression in inflammation and tumor cells (6,7). COX-2 leads to increased synthesis and secretion of prostaglandin E2 (PGE2), which in turn activates cell growth and inhibits apoptosis (8). COX-2 is associated with the occurrence and progression of various cancer types (9), including squamous cell carcinoma, cholangiocarcinoma, endometrial carcinoma and hepatocellular carcinoma. COX-2 regulates the transcription of EGFR through transcriptional activator protein-1 (10). It also plays a role in the process of drug resistance (11,12). Celecoxib, a COX-2 specific inhibitor, is one of the most widely used and promising drugs for cancer therapy (13). However, little research has been conducted on its use in the treatment of renal cancer. The objective of the present study was to investigate whether the combination of celecoxib may improve the efficacy of sorafenib in the treatment of RCC.

A stress granule (SG) is a highly dynamic membrane-free structure in cells that contains mRNA encoding stress-adaptive proteins and a variety of RNA-binding proteins (RBPs), including Ras GTPase-activating protein-binding protein 1 (G3BP1), human antigen R (HuR), T-cell-restricted intracellular antigen-1 (TIA-1) and Tristetraprolin (TTP) (14). SGs can redistribute intracellular resources under stress conditions, stabilize mRNA and regulate expression of genes that promote cell survival (14,15). In tumor cells, SGs can promote cell resistance to stress and promote tumor survival and progression (16,17). Several SG components have been found to be overexpressed in tumors, and their expression levels can be used to predict clinical outcomes (18,19). In addition, previous studies have shown that SGs may confer chemotherapy resistance to tumor cells (20,21). It has been reported that COX-2 mRNA can be captured by SGs (22). SGs represent a novel target for developing therapies to suppress COX-2 protein expression. It will also be important to study the role of SGs on the expression of other genes involved in tumor pathogenesis. In the present study, the efficacy of sorafenib in combination with the COX-2 inhibitor, celecoxib, on renal cancer cells was investigated and the mechanism of COX-2 upregulation induced by sorafenib was explored.

Materials and methods

Cell culture. The 786-O and ACHN renal cancer cell lines were obtained from The Cell Bank of Type Culture Collection of The Chinese Academy of Sciences. 786-O cells were cultured in RPMI 1640 (Wisent Biotechnology) and ACHN cells were cultured in DMEM (Wisent Biotechnology) under standard procedures. All complete media were supplemented with 10% (v/v) FBS (Gibco; Thermo Fisher Scientific, Inc.), 100 U/ml penicillin and 100 μg/ml streptomycin (Wisent Biotechnology) at 37˚C with 5% CO_2.

RNA interference and lentivirus. Small interfering RNAs (siRNAs) of COX-2 and G3BP1 were purchased from Generay Biotech Co., Ltd. The specific siRNA were as follows: COX-2 siRNA-1 sense, 5'-GAGCAGUUGUUCCAGACAATT-3'; COX-2 siRNA-1 antisense, 5'-UUGUCUGGAACAACU GCUCTT-3'; COX-2 siRNA-2 sense, 5'-GAUUGAAGAUUA UGUGCAATT-3'; COX-2 siRNA-2 antisense, 5'-UUGCAC AUAAUCUUCAAUCTT-3'; G3BP1 siRNA-1 sense, 5'-GGA GGAGUCUGAAGAAGAATT-3'; G3BP1 siRNA-1 antisense, 5'-UUCUUCUUCAGACUCCUCCTT-3'; G3BP1 siRNA-2 sense, 5'-GCCUGAGCCAGUAUUAGAATT-3'; G3BP1 siRNA-2 antisense, 5'-UUCUAAUACUGGCUCAGGCTT-3'; Control siRNA sense, 5'-UUCUCCGAACGUGUCACG UTT-3'; Control siRNA antisense, 5'-ACGUGACACGUU CGGAGAATT-3'. ACHN cells were transiently transfected with the siRNAs of target genes and negative control siRNA using INTERFERin (Polyplus-transfection SA). The cells were inoculated in a six-well plate, and when the density was about 30-50%. Diluted 2.2 pmoles of siRNA duplexes into 200 μl of medium without serum. Added 8 μl of INTERFERin to the 200 μl of siRNA duplexes and immediately homogenized by vortexing for 10 sec. Incubated for 10 min at room temperature. Added 2 ml of fresh pre-warmed complete medium and 200 μl of transfection mix per well and incubated the plate at 37˚C. Changed to fresh medium after 12 h and continued to culture for 24 or 48 h. G3BP1 short hairpin RNA (shRNA) and control shRNA lentivirus were purchased from Shanghai GeneChem, Co., Ltd. The sequences of the shRNA was as follows: G3BP1 shRNA, CCTGATGATTCTGGAACTT; Control shRNA, TTCTCCGAACGTGTCACGT. The plasmid information is hU6-MCS-Ubiquitin-firefly_Luciferase-IRES-puromycin. ACHN cells (MOI: 15) were inoculated in 12-well plate and transduced with lentivirus (Virus titer: G3BP1 shRNA, 4.5E+08T U/ml; Control shRNA, 3.0E+08T U/ml.) after the density reached 20%. Added 3 μl of G3BP1 shRNA lentivirus or 4.5 μl of control shRNA lentivirus, 20 μl of cotransfection reagent HitransG P (GeneChem, Co., Ltd.) and 500 μl of fresh medium per well and incubated the plate at 37˚C. Changed to complete culture medium after 10 h. After 48 h of transfection, 2 μg/ml puromycin (Thermo Fisher Scientific, Inc.) was used to select for positively transfected cells. After 7 days of selection with puromycin, the surviving cells were used to determine the knockdown efficiency.

Reverse transcription-quantitative PCR (RT-qPCR). Total RNA was isolated from ACHN and 786-O cells using TRIzol (Vazyme Biotech Co., Ltd.). Reverse transcriptions were performed using HiScript RT SuperMix (Vazyme Biotech Co., Ltd.). The procedure was as follows: 50˚C for 15 min; 85˚C for 5 sec; 4˚C for 10 sec. qPCR was performed using ChamQ Universal SYBR qPCR Master Mix (Vazyme Biotech Co., Ltd.), on an ABI QuantStudio 6 Flex Real-Time PCR System (Thermo Fisher Scientific, Inc.). The PCR was as follows: 95˚C for 30 sec and 45 cycles of 95˚C for 10 sec; 60˚C for 30 sec. The fold change of the mRNA levels was calculated using the $2^{-\Delta\Delta Cq}$ method. The specific primers were as follows: COX-2 forward, 5'-CTATCACTGGCATCCCCTTCT-3'; COX-2 reverse, 5'-CTTTCTGTACTGCGGGTGGAA-3'; G3BP1 forward, 5'-AGAGGTGAGGTCCGTCTGAA-3'; G3BP1 reverse, 5'-TTATCTCGTCGGTCGCCTTC-3'; actin forward, 5'-CATGTACGTTGCTATCCAGGC-3'; actin reverse, 5'-CTC CTTAATGTCACGCACGAT-3'.

Antibodies. Antibodies against G3BP1 (WB, 1:1,000; IF, 1:300; cat. no. 13057-2-AP) and HuR (IF, 1:300; cat. no. 66549-1-Ig) were from Proteintech Group, Inc. The antibody against COX-2 (WB, 1:1,000; cat. no. 12282S) was from Cell Signaling Technology, Inc. Goat anti-Rabbit IgG (H+L) Highly Cross-Adsorbed Alexa Fluor 488 secondary antibody (IF, 1:800; cat. no. A32731) and Goat anti-Mouse IgG (H+L) Cross-Adsorbed Alexa Fluor 594 Secondary Antibody (IF, 1:800; cat. no. A11005) were from Thermo Fisher Scientific, Inc. Anti-rabbit IgG, HRP-linked Antibody (WB, 1:2,000; cat. no. 7074S) and Anti-mouse IgG, HRP-linked Antibody (WB, 1:2,000; cat. no. 7076S) were from Cell Signaling Technology, Inc.

Western blotting. Total cell extracts were lysed on ice using a lysis buffer (containing proteinase and phosphatase inhibitors; Beyotime Biotech Co., Ltd.). Protein concentrations were measured using the BCA Kit (Vazyme Biotech Co., Ltd.). Samples were mixed with SDS-PAGE Sample Loading Buffer (5X, Beyotime Biotech Co., Ltd.) and denatured at 95˚C for 5 min, then resolved on 10% gels using SDS-PAGE in running

buffer (Sangon Biotech Co., Ltd. Tris, 3 g; Glycine, 14.4 g; SDS, 1 g; Fix the volume to 1 liter with DD water.). Proteins were transferred to polyvinylidene difluoride (PVDF) membranes (Bio-Rad Laboratories, Inc.). After blocking with 5% skimmed milk at room temperature for 1 h, the PVDF membranes were incubated with primary antibodies at 4˚C overnight, washed with PBST and then incubated with secondary antibodies at room temperature for 1 h. After washing with PBST 3 times, signals were detected using an enhanced chemiluminescence system (Vazyme Biotech Co., Ltd.) and acquired by ChemiScope 3300 Mini Imaging System (Clinx Science Instruments Co., Ltd.).

Immunofluorescence (IF). ACHN and 786-O cells were fixed with 4% paraformaldehyde for 15 min at room temperature, then washed with PBS 3 times and permeabilized with 0.3% Triton X-100 for 20 min at room temperature. Samples were blocked with 3% BSA (Sangon Biotech Co., Ltd.) for 30 min at room temperature and incubated with specific primary antibodies overnight at 4˚C in 3% BSA. After washing, the fluorescently labelled secondary antibodies were incubated for 1 h at room temperature. After further washing, nuclei were stained with DAPI at room temperature for 10 min. Slides were observed and imaged using the EVOS FL Auto 2.0 Imaging System (Thermo Fisher Scientific, Inc.).

MTT assay. Cell viability was measured using an MTT assay. ACHN cells in logarithmic phase were cultured in 96-well plates ($4x10^3$ cells per well). Cells were exposed to sorafenib and celecoxib (Selleck Chemicals) at the indicated concentration for 48 h. After discarding the cell culture media, cells were washed and then incubated in 0.5 mg/ml MTT (Sangon Biotech Co., Ltd.) for 2 h at 37˚C. MTT crystals were dissolved in DMSO (Sangon Biotech Co., Ltd.). The absorbance per well was proportional to the cell viability. The absorption value was measured at a wavelength of 490 nm using the infinite M200Pro system (Tecan Group, Ltd.).

Cell apoptosis. Cell apoptosis was detected using the annexin V-Alexa Fluor 647/propidium iodide double staining method. The adherent ACHN cells were digested and collected after drug treatment. The cells were washed and resuspended with 1X binding buffer (Yeasen Biotech Co., Ltd.). Annexin V-Alexa Fluor 647 and propidium iodide staining solution (Yeasen Biotech Co., Ltd.) were added. A total of 10,000 cells per sample were analyzed by flow cytometry (NovoCyte, 2060R, ACEA Bioscience, Inc.; Agilent) following the reaction at room temperature and avoiding light. The data were analyzed using FlowJo v10 (FlowJo LLC).

RNA fluorescence in situ hybridization (FISH). COX-2 mRNAs were detected using FISH mixed probe (RIBO Biotech Co., Ltd.) and an RNAScope kit (RIBO Biotech Co., Ltd.). The ACHN cells were aliquoted into 8-well chamber slides and treated with 20 μM sorafenib for 1.5 h when the cell density reached 60%. Except for sorafenib, the treatment of the control group was the same as that for the experimental group. Then cells were fixed with 4% paraformaldehyde for 20 min at 4˚C. After permeation with 0.3% Triton X-100 for 15 min at room temperature and pre-hybridization with prehybridized buffer (RIBO Biotech Co., Ltd.) for 30 min at 37˚C, the *COX-2* mRNA mixed probes were added and incubated at 45˚C overnight. Then, slides were washed with washing buffer (RIBO Biotech Co., Ltd.) at 45˚C and incubated with G3BP1 antibody at 4˚C overnight, and then the goat anti-Rabbit IgG (H+L) Highly Cross-Adsorbed Alexa Fluor 488 secondary antibody and goat anti-Mouse IgG (H+L) Cross-Adsorbed Alexa Fluor 594 secondary antibody at room temperature for 1 h. Nuclei were stained with DAPI at room temperature for 10 min. The slides were observed and imaged using the EVOS FL Auto 2.0 Imaging System.

Actinomycin D (Act D) chase experiment. ACHN cells were treated with 10 μM sorafenib for 2 h to upregulate the mRNA levels of *COX-2* and then washed with PBS twice before 5 μg/ml Act D (Sigma-Aldrich; Merck KGaA) was added. After pre-incubation with Act D for 30 min, cells were additionally treated for the indicated times (2 and 4 h) with vehicle or with sorafenib. At the indicated time, the cells were harvested and total RNA was extracted. RT-qPCR was used to detect the *COX-2* mRNA levels.

Xenograft tumor models. Male nude mice (4-6 weeks old, weighing 20.1±1.8 g) were purchased from GemPharmatech. The animal experiments were approved by The Ethical Committee of Nanjing Drum Tower Hospital (Medical School of Nanjing University, Nanjing, China; project ID, 2021-640-01) and were conducted in accordance with The National Institute of Health Guide for the Care and Use of Laboratory Animals and The Institutional Animal Care and Use Committee of Nanjing Drum Tower Hospital. Mice were raised in pathogen-free animal facilities at 20-24˚C, 50% relative humidity and 12 h of light and dark cycle. Mice had free access to water and food, and the health and behavior of the animals were monitored every day. In the *in vivo* experiment of drug combination (n=6), ACHN cells ($3x10^6$ cells in 100 μl PBS) were inoculated subcutaneously in the right flank of each mouse. One week after tumor implantation, the tumor volume of mice reached >50 mm^3, mice were randomized and divided into four groups with similar starting mean tumor volumes: Control, Sorafenib (30 mg/kg), Celecoxib (50 mg/kg), sorafenib (30 mg/kg) plus celecoxib (50 mg/kg). The medicine was given by intragastric administration three times a week for 22 days. In the *in vivo* experiment of administration after knocking down G3BP1 (n=7), the mice were divided into four groups: $ACHN^{CtrlKD}$ with control treatment, $ACHN^{CtrlKD}$ with sorafenib (30 mg/kg) treatment, $ACHN^{G3BP1KD}$ with control treatment, $ACHN^{G3BP1KD}$ with sorafenib (30 mg/kg) treatment. The lentivirus knockdown stable cell line $ACHN^{G3BP1KD}$ and control cell line $ACHN^{CtrlKD}$ were amplified and $4x10^6$ cells were suspended in 100 μl PBS and inoculated subcutaneously in the right flank of each mouse. One week after tumor implantation, the tumor volume of mice reached >50 mm^3, at which time the medicine was given to the mice. The medicine was given by intragastric administration three times a week for 16 days. Considering animal welfare, action should be taken to reduce the pain of animals. The mice were euthanized with intraperitoneal injection of 60 mg/kg pentobarbital followed by rapid cervical dislocation. Mice were judged to be dead if they

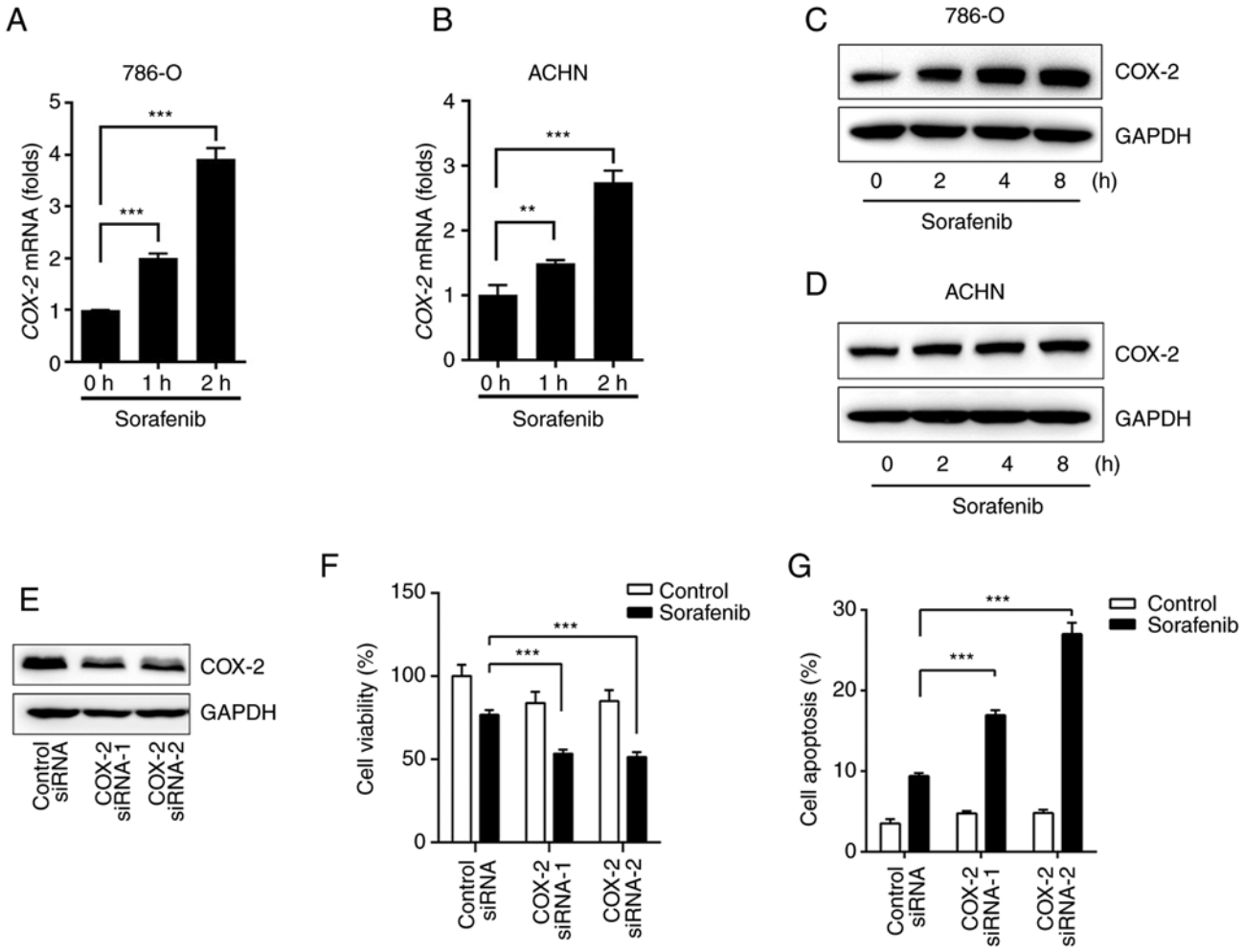

Figure 1. Involvement of COX-2 in sorafenib-induced cell death. (A) 786-O and (B) ACHN cells were treated with 10 μM sorafenib for the indicated times and *COX-2* mRNA was examined by reverse transcription-quantitative PCR analysis. COX-2 protein levels in (C) 786-O and (D) ACHN cells were examined by immunoblot analysis. (E) Western blot analysis of ACHN cells transfected with siRNAs against COX-2. (F) Control or COX-2-silenced ACHN cells were treated with 10 μM sorafenib for 48 h and the cell viability was examined by MTT assay. (G) After treatment, cell apoptosis was detected by flow cytometry. Data represent mean ± SD. **P<0.01, ***P<0.001. COX-2, cyclooxygenase-2; siRNA, small interfering RNA.

were not breathing and did not exhibit nerve reflexes. Tumor volume was calculated using the formula: V=½ x L x W^2, where L is the maximum diameter and W is the minimum diameter of the tumor.

Statistical analysis. All data were presented as mean ± SD. Two group comparisons were performed by unpaired Student's t-test. Statistical analyses involving multiple group comparisons were performed using one-way ANOVA followed by Dunnett's or Tukey's post hoc test. All data analyses were performed with GraphPad Prism 7 (Dotmatics). P<0.05 was considered to indicate a statistically significant difference.

Results

COX-2 expression levels determine sensitivity of renal cancer cells to sorafenib. By examining COX-2 levels before and after sorafenib treatment, it was found that sorafenib rapidly increased mRNA and protein levels of COX-2 in ACHN and 786-O cells (Fig. 1A-D). COX-2 plays a crucial role in the progression of renal cancer (23) and a previous study has suggested that COX-2 decreases the sensitivity of sorafenib in hepatocellular carcinoma (24). In the present study, it was found that the cytotoxicity of sorafenib was affected by the presence of COX-2. After the silencing of COX-2 (Fig. 1E), the specificity effect of COX-2 was indicated by the significant attenuation of ACHN cell survival after sorafenib treatment (Fig. 1F). By using flow cytometry analysis, sorafenib-induced apoptosis was also notably increased in ACHN cells after the silencing of COX-2 expression (Figs. 1G and S1A).

Celecoxib enhances the cytotoxicity of sorafenib against RCC. Increasing evidence has implied that COX-2 inhibitors have potent antitumor effects (9). A case report has also described 2 desmoid tumor patients with multiple recurrences after a combination medical and surgery, who had a major objective response to a combination therapy of celecoxib and sorafenib (25). These findings highlight the possibility that celecoxib may enhance the response to sorafenib in renal cancer. To assess the effect of sorafenib and celecoxib on the viability of human renal cancer cells, dose-dependent inhibition of cell activity with sorafenib and celecoxib was conducted. Cell viability was significantly inhibited after 48 h of sorafenib treatment when the dose exceeded 8 μM (Fig. 2A).

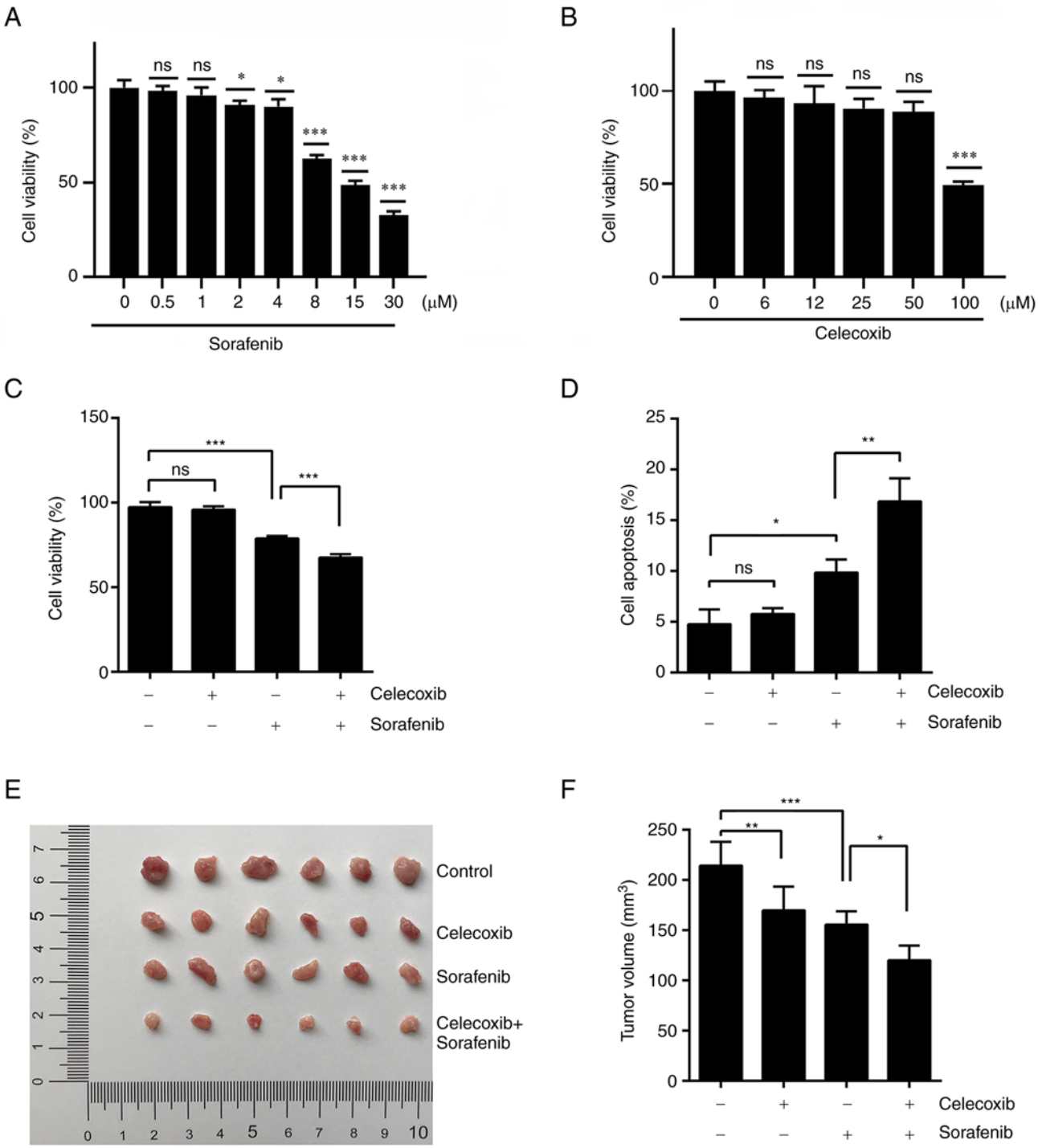

Figure 2. Celecoxib in combination with sorafenib for the treatment of renal cell carcinoma. (A) ACHN cells were treated with sorafenib for 48 h at 0, 0.5, 1, 2, 4, 8, 15 and 30 μM. (B) ACHN cells were treated with celecoxib for 48 h at 0, 6, 12, 25, 50 and 100 μM. Cell viability was examined by MTT assay and the viability of untreated cells was arbitrarily set at 100%. (C) ACHN cells were treated with 30 μM celecoxib, 10 μM sorafenib or 30 μM celecoxib + 10 μM sorafenib for 48 h. Cell viability was examined by MTT assay. (D) Cell apoptosis was detected by flow cytometry. (E) Nude mice were randomized and divided into four groups with similar starting mean tumor volumes. The groups were: Control, 30 mg/kg sorafenib, 50 mg/kg celecoxib and 30 mg/kg sorafenib + 50 mg/kg celecoxib. Tumors were resected and measured after 22 days of drug treatment. (F) Statistical Analysis of tumor Volume in (E). Data represent mean ± SD. *P<0.05, **P<0.01, ***P<0.001. ns, not significant.

Celecoxib had no significant effect on cell viability within 50 μM (Fig. 2B). Thus, 10 μM sorafenib and 30 μM celecoxib were selected for combination therapy using dosage *in vitro*. In the MTT assay, the combination of sorafenib and celecoxib displayed significantly increased cytotoxicity compared to sorafenib alone (Fig. 2C). This synergy also occurred when celecoxib was applied in combination with sorafenib during cell apoptosis experiments (Figs. 2D and S1B).

To confirm the synergistic effect of the combination therapy *in vivo*, nude mice were inoculated with ACHN cells to produce tumor-bearing models. Consistent with the previous *in vitro* results, combined celecoxib and sorafenib treatments

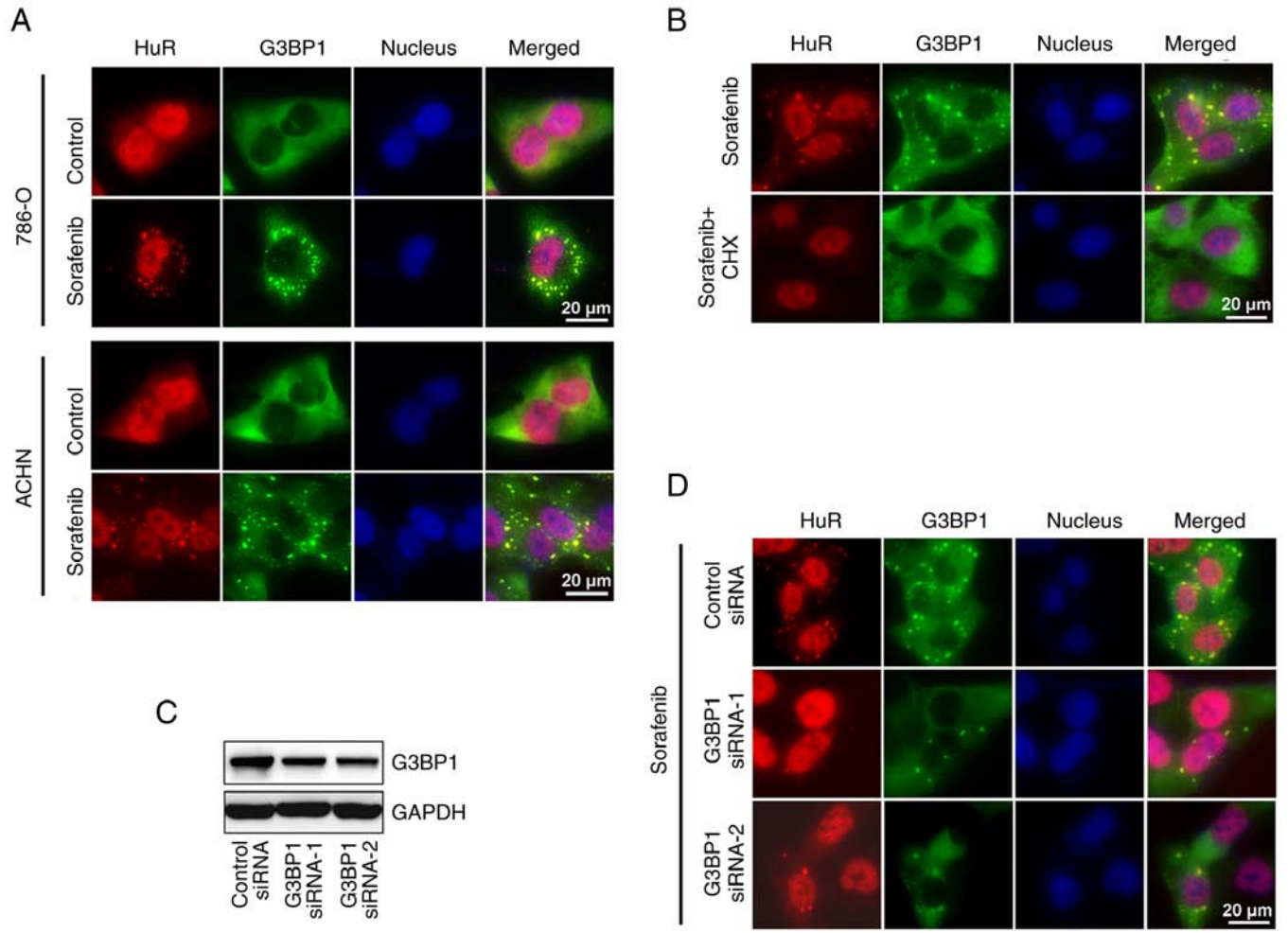

Figure 3. Sorafenib induces assembly of SGs in renal cancer cells. (A) ACHN cells were treated or untreated with 20 μM sorafenib for 1.5 h, and SGs were visualized by immunofluorescence staining with antibodies specific to HuR and G3BP1. (B) Cells were treated with 20 μM sorafenib or 20 μM sorafenib + 2 μM CHX for 1.5 h. Antibodies against HuR and G3BP1 were used to analyze SG assembly. (C) Cells were transfected with G3BP1 or control siRNA for 48 h. The expression of G3BP1 was detected by western blotting. (D) After knocking down G3BP1, cells were treated with 20 μM sorafenib for 1.5 h, followed by immunofluorescent staining with antibodies specific to HuR and G3BP1. The nuclei were visualized using DAPI. Scale bar, 20 μm. CHX, cycloheximide; G3BP1, Ras GTPase-activating protein-binding protein 1; HuR, human antigen R; SG, stress granule; siRNA, small interfering RNA.

significantly slowed the tumor growth of ACHN xenografts compared with sorafenib alone (Fig. 2E). An analysis of the tumors removed after experiments demonstrated that combined celecoxib and sorafenib treatments resulted in a significant decrease in tumor volume compared with sorafenib alone (Fig. 2F). Overall, these results demonstrated that the combination of celecoxib and sorafenib lead to a significant synergistic effect on tumor growth inhibition.

Sorafenib induces the formation of SGs. The mechanism by which sorafenib upregulates COX-2 expression was further explored. It was observed that sorafenib can induce HuR translocation to the cytoplasm and the formation of numerous small foci in the cytoplasm. Using IF analysis, it was observed that these foci were co-localized with SG markers, HuR and G3BP1 (Fig. 3A). The formation of these small cytoplasmic foci was inhibited in cells treated with the SG inhibitor, cycloheximide (Fig. 3B), and they were therefore finally characterized as SGs.

SGs are assembled by liquid-liquid phase separation, which results from unevenly distributed interactions across the core protein-RNA network. G3BP1 is the central protein of this network (26). In the present study, ACHN cells were transfected with specific siRNA to knockdown G3BP1 expression (Fig. 3C). As expected, the formation of SGs was inhibited in cells with a decreased expression of G3BP1 (Fig. 3D).

SGs sequester and stabilize COX-2 mRNA in renal cancer cells. SGs contain translationally stalled mRNAs and RBPs, such as HuR, which bind to mRNAs and modulate their stability (22). Treatment of renal cancer cells with sorafenib resulted in a rapid upregulation of *COX-2* mRNA (Fig. 1A and B). A corresponding increase in the COX-2 protein level was also detected only 2 h after sorafenib treatment (Fig. 1C and D). A previous study has reported that *COX-2* mRNA can be sequestered by SGs (22). To determine whether the increase in COX-2 in sorafenib-treated renal cancer cells was due to the stabilization of *COX-2* mRNA by SGs, sorafenib-treated cells were examined by FISH of *COX-2* mRNA and IF of G3BP1 protein. Subsequently, granular distribution of *COX-2* mRNA was notably co-localized with G3BP1 protein (Fig. 4A).

Of note, sorafenib-enhanced *COX-2* mRNA levels were significantly suppressed after interfering with SG formation

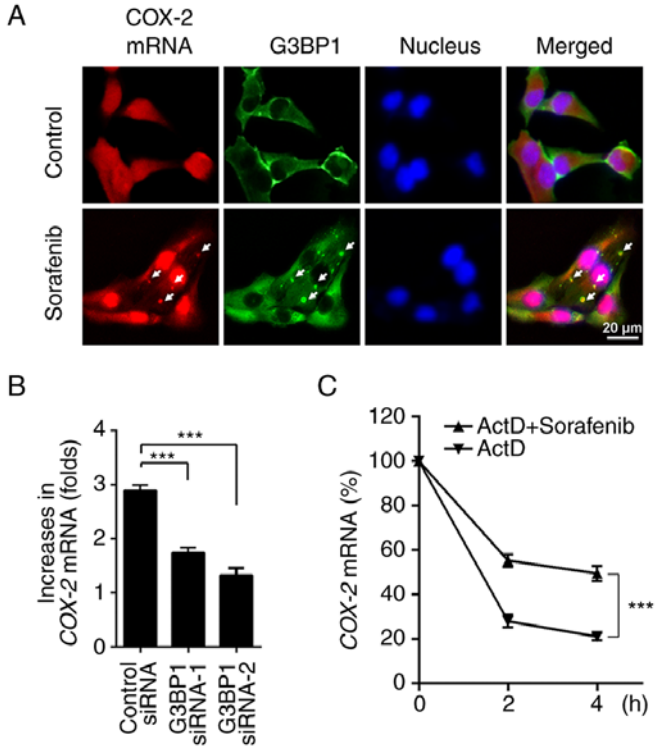

Figure 4. *COX-2* mRNA sequestered in SGs and levels increased in sorafenib-treated renal cancer cells. (A) ACHN cells were seeded in 8-well chamber slides and treated with 20 μM sorafenib for 1.5 h. RNA fluorescence *in situ* hybridization analysis of *COX-2* mRNA and co-immunostaining of G3BP1 was conducted. Scale bar, 20 μm. (B) Control or G3BP1-silenced ACHN cells were treated with 10 μM sorafenib for 2 h, and *COX-2* mRNA expression was examined by RT-qPCR. (C) Detection of *COX-2* mRNA stability before and after sorafenib treatment. The *COX-2* mRNA levels were quantified by RT-qPCR using actin as the normalization control. Data represent mean ± SD. ***P<0.001. Act D, actinomycin D; COX-2, cyclooxygenase-2; G3BP1, Ras GTPase-activating protein-binding protein 1; RT-qPCR, reverse transcription-quantitative PCR; siRNA, small interfering RNA.

by knocking down G3BP1 (Fig. 4B). This result demonstrated that SGs were required for the upregulation of COX-2 induced by sorafenib. The effect of SGs on the stability of *COX-2* mRNA was analyzed using 5 ug/ml Act D. ACHN cells were treated with sorafenib for 2 h to allow the upregulation of *COX-2* mRNA. After pre-incubation with Act D, cells were additionally treated with vehicle or sorafenib, and then the *COX-2* mRNA levels were determined at the indicated times. The half-life of *COX-2* mRNA in renal cancer cells increased after sorafenib treatment and the decay of *COX-2* mRNA was prevented by sorafenib therapy (Fig. 4C). These findings support the suggestion that sorafenib upregulates COX-2 expression as its mRNA is sequestrated and stabilized by SGs.

SGs protect cells from sorafenib-induced cell death. To examine whether SG formation protects cancer cells, silencing of G3BP1 expression in ACHN cells was performed to disrupt SG formation (Fig. 3D). Silencing G3BP1 markedly promoted sorafenib-induced cell death (Fig. 5A). In addition, sorafenib-induced cell apoptosis increased after the expression of G3BP1 decreased (Figs. 5B and S1C).

To confirm the protective effect of SGs *in vivo*, G3BP1 expression was stably knocked down in ACHN cells to obtain ACHN^{G3BP1KD} cells alongside control ACHN^{CtrlKD} cells, and then their response to sorafenib was tested. The cells were inoculated into nude mice to produce tumor-bearing models. Knockdown of G3BP1 significantly suppressed the tumor growth of ACHN xenografts (Fig. 5C). In addition, sorafenib treatment of ACHN^{G3BP1KD} cells resulted in a marked reduction in tumor volume compared with the treatment of ACHN^{CtrlKD} cells (Fig. 5D). Overall, these data suggest that sorafenib-induced SGs have a protective effect on renal cancer cells.

Discussion

COX-2 has been reported to modulate the sensitivity of sorafenib to liver cancer (24). In the present study, it was demonstrated that sorafenib rapidly upregulated COX-2 expression, which decreased the sensitivity of renal cancer cells to sorafenib. COX-2 inhibitors have potent antitumor effects (27). Therefore, the COX-2 inhibitor, celecoxib, in combination with sorafenib in the treatment of RCC was explored. In both cell and animal experiments, it was demonstrated that the combination therapy was significantly better than sorafenib alone in the treatment of RCC. Moreover, it was demonstrated that sorafenib could induce the formation of SGs in renal cancer cells, and the upregulation of COX-2 expression was dependent on the formation of SGs. SGs are membrane-free structures in cells that selectively protect and stabilize pro-survival mRNAs, and it has been reported that *COX-2* mRNA can be captured by SGs (22). In the present study, it was demonstrated that *COX-2* mRNA colocalized with sorafenib-induced SGs in the cytoplasm and the half-life of *COX-2* mRNA was significantly increased after sorafenib treatment. Disruption of SG formation by knocking down G3BP1 expression significantly promoted the cytotoxicity of sorafenib in renal cancer. These results indicate that sorafenib can selectively stabilize mRNAs by inducing SG formation, subsequently increasing the level of COX-2 and the viability of renal cancer cells. Therefore, a regulatory mechanism for the effect of sorafenib on COX-2 levels has been uncovered and new light has been shed on renal cancer therapy.

COX-2 commonly exerts a role in promoting cancer (28-30). For example, COX-2 is a well-known promoter of proliferation, angiogenesis, apoptosis inhibition and immune suppression in melanoma (31). COX-2 expression in breast cancer is associated with the increase of blood vessels and the elevated expression of the angiogenesis marker, VEGF (32,33). COX-2 also plays an essential role in the progression of renal cancer (23,34). In the present study, it was found that sorafenib rapidly and significantly increased COX-2 expression in RCC cells. COX-2 has also previously been found to be important in tumor immunosuppression and is associated with lower infiltration of immune cells in melanoma tissues and a shorter survival time (35,36). The COX-2/mPGES1/PGE2 pathway can regulate the expression of PD-L1 in tumor-associated macrophages and myeloid-derived suppressor cells (30). Immunotherapy offers new hope for patients with cancer. However, the mechanisms of immune regulation in the renal tumor microenvironment and their interaction with molecularly targeted therapeutic agents require further investigation.

COX-2 also exerts a crucial role in the promotion of cancer cell resistance to chemotherapy (9). In the present study, it

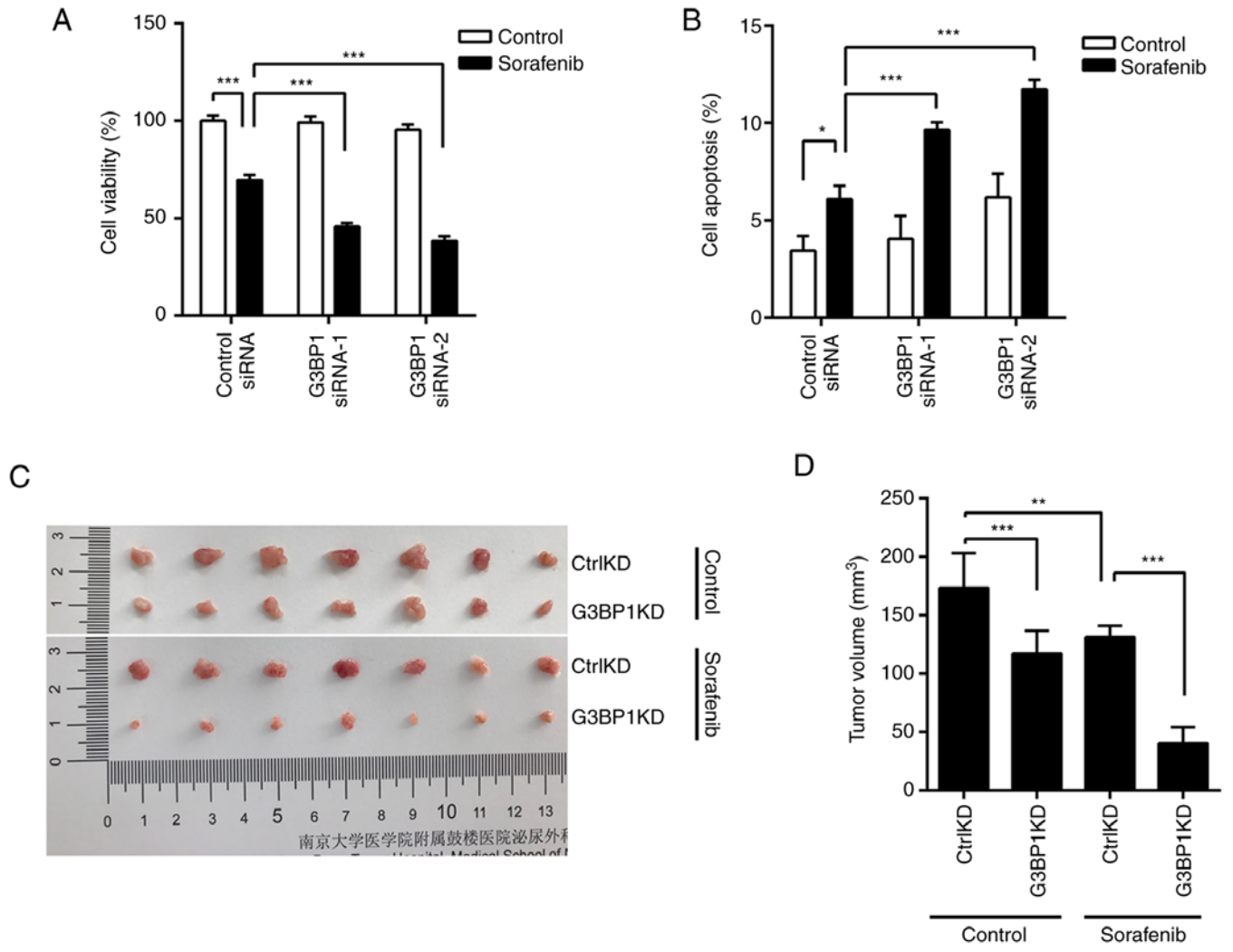

Figure 5. SGs protect renal cancer cells from sorafenib-induced cell death. (A) Control or G3BP1-silenced ACHN cells were treated with 10 μM sorafenib for 48 h and cell viability was examined by MTT assay. (B) After treatment, cell apoptosis was detected by flow cytometry. (C) Nude mice were randomized and divided into four groups with similar starting mean tumor volumes: $ACHN^{CtrlKD}$ with control treatment, $ACHN^{CtrlKD}$ with 30 mg/kg sorafenib treatment, $ACHN^{G3BP1KD}$ with control treatment, $ACHN^{G3BP1KD}$ with 30 mg/kg sorafenib treatment. Tumors were resected and measured after 16 days of drug treatment. (D) Statistical Analysis of tumor Volume in (C). Data represent mean ± SD. *P<0.05, **P<0.01, ***P<0.001. ns, not significant. Ctrl, control; KD, knockdown; G3BP1, Ras GTPase-activating protein-binding protein 1; siRNA, small interfering RNA.

was demonstrated that the upregulated expression of COX-2 promoted the survival of renal cancer cells and decreased the cytotoxicity of sorafenib. These results highlight the high potential of the COX-2 inhibitor, celecoxib, in the treatment of renal cancer, particularly for enhancing the response to sorafenib. In mice bearing human RCC xenografts, COX-2 inhibition can extend the therapeutic effect of the VEGFR inhibitor, sunitinib (37). Celecoxib combined with sorafenib significantly inhibited proliferation and induced apoptosis of hepatocellular carcinoma cells (38). A combined treatment of sorafenib and celecoxib had a more notable tumor suppression effect than the single drug group in mice with lung cancer (39). In the present study, it was demonstrated that the combined treatment with celecoxib significantly enhanced the cytotoxicity of sorafenib on renal carcinoma cells. COX-2 inhibitors are inexpensive, have tolerable side effects and can sensitize cancer cells to chemotherapy (40). A single-center randomized controlled clinical phase III trial recommended celecoxib for the mitigation of sorafenib-related skin toxicity in patients with hepatocellular carcinoma (41). Longer PFS was achieved in the celecoxib + sorafenib combination group, although overall survival time was not prolonged in clinical practice. Clinical trials combining celecoxib and sorafenib to delay the progression of renal cancer should therefore be considered.

Sorafenib can act on both wild-type and V599E mutant RAF (42). The level of VEGFR/PDGFR is still inhibited in RCC after sorafenib treatment (43). However, Some compensatory signaling pathways such as PI3K-AKT-mTOR can promote renal cell survival and cancer progression (44). To the best of our knowledge, there is still no marker that predicts renal cancer response to drug therapy. Sorafenib treatment creates a pressure environment and the surviving cancer cells are more aggressive (45). This adaptation requires cancer cells to survive through their own stress response mechanisms. The formation of SGs is a mechanism for minimizing stress damage and increasing cell survival. SGs participate in inflammatory and apoptotic signaling and promote cell survival (46,47). Sorafenib also promotes SG production in various cancer

cells, including HeLa, MCF-7, PC3 and LnCaP cells (48). In the present study, it was found that sorafenib could induce the assembly of SGs in renal cancer cells. Moreover, these SGs protected and promoted the survival of renal cancer cells by selectively stabilizing *COX-2* mRNA and promoting its expression. SG proteins are involved in processes of translation and mRNA stability. Targeting SGs may be a novel method of treating disease (49). The specific mechanism of sensitivity of renal cancer cells to sorafenib, which is regulated by SGs, needs further exploration as targeting SGs may be a potential therapeutic strategy for renal cancer therapy.

However, There are inevitably some limitations to the present study. In the *in vitro* study, normal renal cancer cells were used to conduct cell sensitivity experiments after drug treatments. If the normal renal cancer cells were replaced with cell lines resistant to sorafenib, it may be closer to the physiological conditions of drug resistance. In the *in vivo* study, it was demonstrated that celecoxib combined with sorafenib can inhibit the growth of subcutaneous tumors in nude mice. However, there was a lack of exploration of the molecular mechanism behind this drug combination. In the molecular mechanism study, it was demonstrated that SGs can stabilize COX-2 mRNA. However, it is worth noting that SGs may also play different roles by regulating the mRNA stability of other molecules, which requires a more in-depth study.

In summary, sorafenib is an identified drug that can upregulate COX-2 levels in renal cancer cells. COX-2 promotes the survival of renal cancer cells. The use of celecoxib, a COX-2 inhibitor, in combination with sorafenib significantly enhanced the sensitivity of renal cancer cells to sorafenib and improved efficacy. Clinical trials of celecoxib in combination with sorafenib for the treatment of renal cancer should be considered. In the present study, a novel regulatory mechanism for COX-2 expression was uncovered. Sorafenib-induced assembly of SGs in renal cancer cells is a critical event that promotes COX-2 expression and acts as a stress mechanism against treatment. Therefore, the assembly of SGs and their role in regulating the expression of different oncogenes is crucial for additional exploration. The findings of the present study may provide novel targets for the treatment of renal cancer.

Acknowledgements

Not applicable.

Funding

This work was supported by The National Natural Science Foundation of China (grant no. 81972387) and The Nanjing Health Distinguished Youth Fund (grant no. JQX20002).

Availability of data and materials

The datasets used and/or analyzed during the current study are available from the corresponding author on reasonable request.

Authors' contributions

HQD, GLW, WMC, WQ, WC and HQG confirm the authenticity of all the raw data. HQG and WC participated in the conception and design of the study. HQD and GLW performed all the experiments with help from WMC and WQ. WC and HQG wrote the manuscript, performed the statistical analyses and evaluated the results. All authors read and approved the final manuscript.

Ethics approval and consent to participate

The study was approved by The Ethical Committee of Nanjing Drum Tower Hospital (Medical School of Nanjing University, Nanjing, China; project ID, 2021–640-01), and all experiments involving mice were conducted in accordance with The National Institute of Health Guide for the Care and Use of Laboratory Animals and The Institutional Animal Care and Use Committee of Nanjing Drum Tower Hospital.

Patient consent for publication

Not applicable.

Competing interests

The authors declare that they have no competing interests.

References

1. Sung H, Ferlay J, Siegel RL, Laversanne M, Soerjomataram I, Jemal A and Bray F: Global cancer statistics 2020: GLOBOCAN estimates of incidence and mortality worldwide for 36 cancers in 185 countries. CA Cancer J Clin 71: 209-249, 2021.
2. Capitanio U, Bensalah K, Bex A, Boorjian SA, Bray F, Coleman J, Gore JL, Sun M, Wood C and Russo P: Epidemiology of renal cell carcinoma. Eur Urol 75: 74-84, 2019.
3. Capitanio U and Montorsi F: Renal cancer. Lancet 387: 894-906, 2016.
4. Liu L, Cao Y, Chen C, Zhang X, McNabola A, Wilkie D, Wilhelm S, Lynch M and Carter C: Sorafenib blocks the RAF/MEK/ERK pathway, inhibits tumor angiogenesis, and induces tumor cell apoptosis in hepatocellular carcinoma model PLC/PRF/5. Cancer Res 66: 11851-11858, 2006.
5. Ljungberg B, Albiges L, Abu-Ghanem Y, Bensalah K, Dabestani S, Fernández-Pello S, Giles RH, Hofmann F, Hora M, Kuczyk MA, *et al*: European association of urology guidelines on renal cell carcinoma: The 2019 update. Eur Urol 75: 799-810, 2019.
6. Sano Y, Kogashiwa Y, Araki R, Enoki Y, Ikeda T, Yoda T, Nakahira M and Sugasawa M: Correlation of inflammatory markers, survival, and COX2 expression in oral cancer and implications for prognosis. Otolaryngol Head Neck Surg 158: 667-676, 2018.
7. Gurram B, Zhang S, Li M, Li H, Xie Y, Cui H, Du J, Fan J, Wang J and Peng X: Celecoxib conjugated fluorescent probe for identification and discrimination of cyclooxygenase-2 enzyme in cancer cells. Anal Chem 90: 5187-5193, 2018.
8. Wu WK, Sung JJ, Lee CW, Yu J and Cho CH: Cyclooxygenase-2 in tumorigenesis of gastrointestinal cancers: An update on the molecular mechanisms. Cancer Lett 295: 7-16, 2010.
9. Hashemi Goradel N, Najafi M, Salehi E, Farhood B and Mortezaee K: Cyclooxygenase-2 in cancer: A review. J Cell Physiol 234: 5683-5699, 2019.
10. Li H, Zhu F, Boardman LA, Wang L, Oi N, Liu K, Li X, Fu Y, Limburg PJ, Bode AM and Dong Z: Aspirin prevents colorectal cancer by normalizing EGFR expression. EBioMedicine 2: 447-455, 2015.
11. Xiao J, Wang F, Lu H, Xu S, Zou L, Tian Q, Fu Y, Lin X, Liu L, Yuan P, *et al*: Targeting the COX2/MET/TOPK signaling axis induces apoptosis in gefitinib-resistant NSCLC cells. Cell Death Dis 10: 777, 2019.
12. Tong D, Liu Q, Wang LA, Xie Q, Pang J, Huang Y, Wang L, Liu G, Zhang D, Lan W and Jiang J: The roles of the COX2/PGE2/EP axis in therapeutic resistance. Cancer Metastasis Rev 37: 355-368, 2018.

13. Khafaga AF, Shamma RN, Abdeen A, Barakat AM, Noreldin AE, Elzoghby AO and Sallam MA: Celecoxib repurposing in cancer therapy: Molecular mechanisms and nanomedicine-based delivery technologies. Nanomedicine (Lond) 16: 1691-1712, 2021.
14. Bley N, Lederer M, Pfalz B, Reinke C, Fuchs T, Glaß M, Möller B and Hüttelmaier S: Stress granules are dispensable for mRNA stabilization during cellular stress. Nucleic Acids Res 43: e26, 2015.
15. Protter DSW and Parker R: Principles and properties of stress granules. Trends Cell Biol 26: 668-679, 2016.
16. Grabocka E and Bar-Sagi D: Mutant KRAS enhances tumor cell fitness by upregulating stress granules. Cell 167: 1803-1813.e12, 2016.
17. Thedieck K, Holzwarth B, Prentzell MT, Boehlke C, Kläsener K, Ruf S, Sonntag AG, Maerz L, Grellscheid SN, Kremmer E, *et al*: Inhibition of mTORC1 by astrin and stress granules prevents apoptosis in cancer cells. Cell 154: 859-874, 2013.
18. Somasekharan SP, El-Naggar A, Leprivier G, Cheng H, Hajee S, Grunewald TG, Zhang F, Ng T, Delattre O, Evdokimova V, *et al*: YB-1 regulates stress granule formation and tumor progression by translationally activating G3BP1. J Cell Biol 208: 913-929, 2015.
19. Gao X, Jiang L, Gong Y, Chen X, Ying M, Zhu H, He Q, Yang B and Cao J: Stress granule: A promising target for cancer treatment. Br J Pharmacol 176: 4421-4433, 2019.
20. Zhao J, Fu X, Chen H, Min L, Sun J, Yin J, Guo J, Li H, Tang Z, Ruan Y, *et al*: G3BP1 interacts with YWHAZ to regulate chemoresistance and predict adjuvant chemotherapy benefit in gastric cancer. Br J Cancer 124: 425-436, 2021.
21. Shi Q, Zhu Y, Ma J, Chang K, Ding D, Bai Y, Gao K, Zhang P, Mo R, Feng K, *et al*: Prostate cancer-associated SPOP mutations enhance cancer cell survival and docetaxel resistance by upregulating Caprin1-dependent stress granule assembly. Mol Cancer 18: 170, 2019.
22. Ansari MY and Haqqi TM: Interleukin-1β induced stress granules sequester COX-2 mRNA and regulates its stability and translation in human OA chondrocytes. Sci Rep 6: 27611, 2016.
23. Kaminska K, Szczylik C, Lian F and Czarnecka AM: The role of prostaglandin E2 in renal cell cancer development: Future implications for prognosis and therapy. Future Oncol 10: 2177-2187, 2014.
24. Dong XF, Liu TQ, Zhi XT, Zou J, Zhong JT, Li T, Mo XL, Zhou W, Guo WW, Liu X, *et al*: COX-2/PGE2 axis regulates HIF2α activity to promote hepatocellular carcinoma hypoxic response and reduce the sensitivity of sorafenib treatment. Clin Cancer Res 24: 3204-3216, 2018.
25. Benech N, Walter T and Saurin JC: Desmoid tumors and celecoxib with sorafenib. N Engl J Med 376: 2595-2597, 2017.
26. Yang P, Mathieu C, Kolaitis RM, Zhang P, Messing J, Yurtsever U, Yang Z, Wu J, Li Y, Pan Q, *et al*: G3BP1 is a tunable switch that triggers phase separation to assemble stress granules. Cell 181: 325-345.e28, 2020.
27. Tołoczko-Iwaniuk N, Dziemiańczyk-Pakieła D, Nowaszewska BK, Celińska-Janowicz K and Miltyk W: Celecoxib in cancer therapy and prevention-review. Curr Drug Targets 20: 302-315, 2019.
28. Sun Y, Dai H, Chen S, Zhang Y, Wu T, Cao X, Zhao G, Xu A, Wang J and Wu L: Disruption of chromosomal architecture of cox2 locus sensitizes lung cancer cells to radiotherapy. Mol Ther 26: 2456-2465, 2018.
29. Tong D, Liu Q, Liu G, Xu J, Lan W, Jiang Y, Xiao H, Zhang D and Jiang J: Metformin inhibits castration-induced EMT in prostate cancer by repressing COX2/PGE2/STAT3 axis. Cancer Lett 389: 23-32, 2017.
30. Prima V, Kaliberova LN, Kaliberov S, Curiel DT and Kusmartsev S: COX2/mPGES1/PGE2 pathway regulates PD-L1 expression in tumor-associated macrophages and myeloid-derived suppressor cells. Proc Natl Acad Sci USA 114: 1117-1122, 2017.
31. Tudor DV, Bâldea I, Lupu M, Kacso T, Kutasi E, Hopârtean A, Stretea R and Gabriela Filip A: COX-2 as a potential biomarker and therapeutic target in melanoma. Cancer Biol Med 17: 20-31, 2020.
32. Lala PK, Nandi P and Majumder M: Roles of prostaglandins in tumor-associated lymphangiogenesis with special reference to breast cancer. Cancer Metastasis Rev 37: 369-384, 2018.
33. Davies G, Salter J, Hills M, Martin LA, Sacks N and Dowsett M: Correlation between cyclooxygenase-2 expression and angiogenesis in human breast cancer. Clin Cancer Res 9: 2651-2656, 2003.
34. Li Z, Zhang Y, Kim WJ and Daaka Y: PGE2 promotes renal carcinoma cell invasion through activated RalA. Oncogene 32: 1408-1415, 2013.
35. Kim SH, Roszik J, Cho SN, Ogata D, Milton DR, Peng W, Menter DG, Ekmekcioglu S and Grimm EA: The COX2 effector microsomal PGE2 synthase 1 is a regulator of immunosuppression in cutaneous melanoma. Clin Cancer Res 25: 1650-1663, 2019.
36. Mao Y, Poschke I, Wennerberg E, Pico de Coaña Y, Egyhazi Brage S, Schultz I, Hansson J, Masucci G, Lundqvist A and Kiessling R: Melanoma-educated CD14+ cells acquire a myeloid-derived suppressor cell phenotype through COX-2-dependent mechanisms. Cancer Res 73: 3877-3887, 2013.
37. Wang X, Zhang L, O'Neill A, Bahamon B, Alsop DC, Mier JW, Goldberg SN, Signoretti S, Atkins MB, Wood CG and Bhatt RS: Cox-2 inhibition enhances the activity of sunitinib in human renal cell carcinoma xenografts. Br J Cancer 108: 319-326, 2013.
38. Cervello M, Bachvarov D, Lampiasi N, Cusimano A, Azzolina A, McCubrey JA and Montalto G: Novel combination of sorafenib and celecoxib provides synergistic anti-proliferative and pro-apoptotic effects in human liver cancer cells. PLoS One 8: e65569, 2013.
39. Zhang H, Li Z and Wang K: Combining sorafenib with celecoxib synergistically inhibits tumor growth of non-small cell lung cancer cells *in vitro* and *in vivo*. Oncol Rep 31: 1954-1960, 2014.
40. Shi L, Xu L, Wu C, Xue B, Jin X, Yang J and Zhu X: Celecoxib-induced self-assembly of smart albumin-doxorubicin conjugate for enhanced cancer therapy. ACS Appl Mater Interfaces 10: 8555-8565, 2018.
41. Chen JC, Wang JC, Pan YX, Yi MJ, Chen JB, Wang XH, Fu YZ, Zhang YJ, Xu L, Chen MS, *et al*: Preventive effect of celecoxib in sorafenib-related hand-foot syndrome in hepatocellular carcinoma patients, a single-center, open-label, randomized, controlled clinical phase III trial. Am J Cancer Res 10: 1467-1476, 2020.
42. Wilhelm SM, Adnane L, Newell P, Villanueva A, Llovet JM and Lynch M: Preclinical overview of sorafenib, a multikinase inhibitor that targets both Raf and VEGF and PDGF receptor tyrosine kinase signaling. Mol Cancer Ther 7: 3129-3140, 2008.
43. Bergers G and Hanahan D: Modes of resistance to anti-angiogenic therapy. Nat Rev Cancer 8: 592-603, 2008.
44. Rini BI and Atkins MB: Resistance to targeted therapy in renal-cell carcinoma. Lancet Oncol 10: 992-1000, 2009.
45. Fulda S, Gorman AM, Hori O and Samali A: Cellular stress responses: Cell survival and cell death. Int J Cell Biol 2010: 214074, 2010.
46. Wippich F, Bodenmiller B, Trajkovska MG, Wanka S, Aebersold R and Pelkmans L: Dual specificity kinase DYRK3 couples stress granule condensation/dissolution to mTORC1 signaling. Cell 152: 791-805, 2013.
47. Arimoto K, Fukuda H, Imajoh-Ohmi S, Saito H and Takekawa M: Formation of stress granules inhibits apoptosis by suppressing stress-responsive MAPK pathways. Nat Cell Biol 10: 1324-1332, 2008.
48. Adjibade P, St-Sauveur VG, Quevillon Huberdeau M, Fournier MJ, Savard A, Coudert L, Khandjian EW and Mazroui R: Sorafenib, a multikinase inhibitor, induces formation of stress granules in hepatocarcinoma cells. Oncotarget 6: 43927-43943, 2015.
49. Wang F, Li J, Fan S, Jin Z and Huang C: Targeting stress granules: A novel therapeutic strategy for human diseases. Pharmacol Res 161: 105143, 2020.